

Dynamics of high-frequency streamers in air

G. V. Naïdis

Institute of High Temperatures, Russian Academy of Sciences, 127412 Moscow, Russia

(Submitted 21 July 1995)

Zh. Éksp. Teor. Fiz. **109**, 1288–1296 (April 1996)

Numerical modeling is used to investigate the dynamics of streamer formation in air in a high-frequency electric field of strength greater than the critical value. The case of high gas pressures, for which the energy exchange rate between electrons and molecules is greater than the field frequency, is considered. The calculations provide the basis for a determination of the dependence of the plasma parameters in the streamer and also of its size and propagation velocity on the external conditions. © 1996 American Institute of Physics. [S1063-7761(96)01604-6]

The development of discharges in high-pressure gases in both static (homogeneous and inhomogeneous) and high-frequency fields is often accompanied by the formation of thin plasma channels—streamers. A streamer is an ionization wave in whose front (the head of the streamer) charge separation occurs and there is an associated increase of the electric field, which leads to intense impact ionization. The theoretical description of streamer dynamics is a very complicated problem that requires the use of numerical methods on account of the strong nonlinearity of the coupling between charged-particle transport processes and the formation of the spatial distribution of the electric field. This problem has been studied most completely for the development of streamers in static homogeneous fields (see Ref. 1 and the references given there). Streamer dynamics in radio frequency (rf) fields, which has its own distinctive features, was analyzed in Refs. 2–4, in which an approach based on solution of an equation for the amplitude of a quasiharmonic field was used. Such an approach is justified provided the plasma parameters cannot change significantly over the period of the rf wave, i.e., provided $\nu_{im} < \omega/2\pi$, where ν_{im} is the maximum value of the ionization frequency (attained in the head of the streamer), and ω is the frequency of the rf radiation. In high-pressure gases subject to strong fields in the centimeter and decimeter ranges, this inequality may be violated. In this case, the description of the streamer development requires more detailed allowance for the variation of the field over times shorter than the period of the rf wave.

In this paper, we use a model of a single rf streamer similar to that used to investigate streamer dynamics in static fields. We consider the initial stage of streamer development in fields with linear polarization. We assume that the streamer length L is small compared with the wavelength λ of the rf wave, $L < \lambda/\pi$, and that the transverse dimension is much less than the thickness of the skin layer. Under these conditions, the electric field E can be calculated in the quasistatic approximation, corresponding to which we have a Poisson equation for the potential:

$$\mathbf{E} = -\nabla U, \quad \nabla^2 U = -4\pi\rho, \quad (1)$$

which has the formal solution

$$U(\mathbf{r}) = U_L(\mathbf{r}) + \int \frac{\rho(\mathbf{r}')}{|\mathbf{r} - \mathbf{r}'|} d\mathbf{r}'. \quad (2)$$

Here $\rho = e(n_p - n_n - n_e)$ is the volume charge density, n_p , n_n , and n_e are the densities of the positive and negative ions and electrons, and U_L is the potential of the applied (external) field. To determine the charged-particle density, we use the diffusion-drift approximation:

$$\begin{aligned} \frac{\partial n_j}{\partial t} + \nabla(n_j V_j) &= F_j + S_j, \\ \mathbf{V}_j &= \mu_j \mathbf{E} - D_j \nabla \ln n_j, \end{aligned} \quad (3)$$

where μ_j and D_j are the mobility and diffusion coefficients for particles of species j , and the terms F_j correspond to the sums of the contributions of the local kinetic processes of formation and destruction of particles (ionization, attachment, electron-ion and ion-ion recombination). The terms S_j describe the formation of charged seed particles ahead of the streamer front by volume photoionization and have the structure

$$S_p(\mathbf{r}) = S_e(\mathbf{r}) = \int \chi \nu_i(\mathbf{r}') n_e(\mathbf{r}') K(|\mathbf{r} - \mathbf{r}'|) d\mathbf{r}', \quad (4)$$

where the factor χ is equal to the ratio of the number of emitted ionizing photons to the number of ionization events, and the function $K(|\mathbf{r} - \mathbf{r}'|)$ describes the transport of the ionizing radiation.

The values of the constants of the processes that occur in F_j are assumed to correspond to the local values of the electric field strength, since the characteristic scale of variation of the plasma parameters is greater than the energy exchange length. We consider conditions under which $\omega \ll \nu_u$, where ν_u is the frequency of energy exchange between the electrons and the molecules. In air, this inequality corresponds to the range $p_0 \lambda \gtrsim 3$ atm·cm (p_0 is the gas pressure corresponding to the temperature 300 K). In this case, the constants of the kinetic processes can follow the variation in time of E . Since over these characteristic streamer development times $\sim 10^{-8}$ – 10^{-7} s there is not sufficient time for the concentration n_m of the gas molecules to change significantly, the space-time variation of the reduced field E/n_m , which determines the values of the constants, is entirely determined

by the change of E . Note that for values of E/n_m not too much greater than the critical value (for which the ionization frequency is equal to the attachment frequency), the effective ionization constant, averaged over the period T of the rf field,

$$\langle K_{\text{eff}} \rangle = \frac{1}{T} \int_0^T [K_i(t) - K_a(t)] dt, \quad (5)$$

where K_i and K_a are the ionization and attachment constants, exceeds by more than an order of magnitude the value K_{eff} corresponding to the rms value of the field (the opposite limiting case $\omega \gg \nu_u$).

As initial condition, we specify distributions of the charged-particle concentrations of the form

$$n_{e0}(\mathbf{r}) = n_{p0}(\mathbf{r}) = n_{em} \exp\{-|\mathbf{r}|^2/r_0^2\} \quad (6)$$

(the choice of n_{em} and r_0 is discussed below). The presence of axial symmetry of the initial distribution makes it possible to solve the system (1), (3) in the two-dimensional formulation in the axisymmetric coordinate (z, r) system, where the z axis is directed along the vector of the electric field.

We shall consider the streamer dynamics at not too low frequencies of the rf field, so that $\langle \nu_{\text{eff}}^0 \rangle = \langle K_{\text{eff}}^0 \rangle n_m \lesssim \omega/2\pi$ (the superscript 0 corresponds to the value of the variable in the unperturbed external field having amplitude E_0). In this case, the characteristic streamer development time is many periods of the rf field, and this leads to the formation of a streamer that is almost symmetric with respect to the $z=0$ plane. As a result, we can restrict the calculations to the region $z \geq 0$, specifying that derivatives of the densities vanish on $z=0$, and also introducing the image of the space charge in the plane $z=0$ for the calculation of the field.

Direct use of the solution of the Poisson equation (2) in calculations on meshes sufficiently fine for a good spatial resolution of the parameters of the streamer plasma requires an unwarranted volume of calculations. Therefore, the expression (2) with external-field potential

$$U_L(\mathbf{r}, t) = E_0 z \cos \omega t. \quad (7)$$

is used only to calculate the potential on the boundaries of the region of calculation, and the solution of Eq. (1) in the interior points is found by iteration. The two-dimensional transport equations (3) are solved by decoupling with respect to the spatial coordinates, and the calculation of the transport in each of the directions is done by means of a modified flux-corrected method⁵ possessing weak numerical diffusion.

We modeled rf streamers for air close to atmospheric pressure. The dependence of the constants of the kinetic processes and the transport coefficients on E/n_m was calculated in accordance with the data of Refs. 6 and 7. To calculate the photoionization term (4), we used a model of bulk photoionization in discharges in air based on experimental results.⁸

The parameters of the initial distribution (6) are determined by the physical formulation of the problem. Thus, in the case of streamer initiation by a single electron in the stage of the development of an electron avalanche in an applied field undistorted by space charge, the avalanche radius is given by

$$r(t) = 2(D_e t)^{1/2}. \quad (8)$$

Such a dependence holds until free-electron diffusion is replaced by ambipolar diffusion, after which the growth of the avalanche radius becomes much slower. If we substitute in (8) the characteristic time for n_e to grow to the value at which the nature of the diffusion changes, $t \sim 20/\langle \nu_{\text{eff}}^0 \rangle$, then we obtain an estimate of the avalanche radius at the onset of streamer formation:

$$r_0 \sim 10(D_e / \langle \nu_{\text{eff}}^0 \rangle)^{1/2}. \quad (9)$$

In the range $E_0/p_0 = 35-60 \text{ kV} \cdot \text{cm}^{-1} \cdot \text{atm}^{-1}$ considered here, the expression (9) gives $p_0 r_0 = 10^{-2}-10^{-1} \text{ atm} \cdot \text{cm}$. However, one can have situations in which the initial radius r_0 differs from the value (9), for example, when the streamer is initiated by laser irradiation. Therefore, in the calculations it is convenient to assume that r_0 is an adjustable external parameter. Other adjustable parameters are the amplitude E_0 and the frequency ω of the applied field, and also the reduced pressure p_0 (or the molecular density n_m). Variation of n_{em} in the expression for the initial distribution (6) in the range $10^9-10^{12} \text{ cm}^{-3}$ does not affect the picture of streamer development and merely shifts the onset of streamer formation relative to the origin of the calculation. We mention once more that we are treating the dynamics of an isolated streamer, i.e., we assume that the distance between neighboring simultaneously developing streamers is large compared with the streamer diameter.

Figure 1 gives the electron density contours at three successive times (only the right-hand half of the streamer, which is symmetric to the left-hand part, is shown). It can be seen that the streamer has a dumbbell shape, expanding from the center to the heads. The distributions of the amplitude values of the electric field and the electron density on the streamer axis (at $r=0$) at these times are shown in Fig. 2. It can be seen that the field at the head, which greatly exceeds the external field, increases weakly with streamer length, while the field in the central part (in the streamer channel) hardly changes with increasing length, remaining somewhat less than the applied field but greater than the critical field. At the same time, the electron density in the channel grows exponentially with the time.

Figure 3 shows the dependence of the streamer velocity $V = dl/dt$ on l , where $l=L/2$ is the distance from the head to the center of the streamer, and L is the total length of the streamer (the distance between the heads). The velocity increases almost linearly with the streamer length; moreover, as the calculations show, the coefficient of proportionality is practically independent of r_0 and ω and is determined by the value of the external field. If the pressure p_0 and E_0 vary identically, the streamer velocity changes in proportion to p_0 .

Figure 3 also gives the results of calculations of V made in the one-dimensional (1D) approximation. This approximation, which is widely used to model streamers in static fields, is as follows. One considers the time variation of the plasma parameters only in the direction of propagation of the streamer (along the z axis). The structure of the streamer in the transverse (radial) direction is assumed to be unchanged;

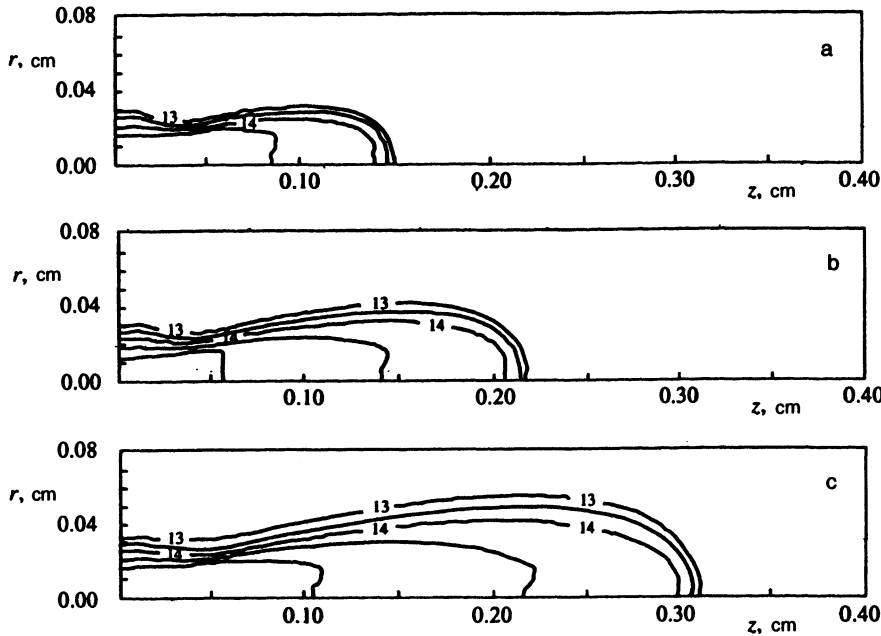


FIG. 1. Electron density contours $E_0=60$ kV·cm; $p_0=1$ atm; $\lambda=9$ cm; $r_0=0.01$ cm. The diagrams give the values of $\log n_e$ [cm^{-3}] at intervals of 0.5 at the times $t=5.1$ (a), 5.7 (b), 6.3 ns (c).

it is assumed that the plasma parameters do not depend on the radial coordinate within a disk that has radius r_0 . Accordingly, the 1D model consists of the system of transport equations (3) in which the flux divergence includes only the derivative with respect to z , and of the expression (2) for the field strength, in which in the integration in the radial direction ρ is assumed to be constant for $r \leq r_0$ and equal to zero for $r > r_0$ (the method of disks). The use of this model appreciably (by 1–2 orders of magnitude) reduces the volume of calculations compared with the more complete two-dimensional model. An obvious shortcoming of the one-dimensional approach is the assumption of constancy of the streamer radius, which, generally speaking, is not satisfied. However, in a number of cases, including (as will be shown below) the one considered in this paper, the 1D model correctly reproduces many features of the phenomenon. Thus, it can be seen from Fig. 3 that this model gives streamer velocities that are close to the results of the two-dimensional calculations.

The results of the calculations show that to a good accuracy the streamer velocity can be described by the relation

$$V = \zeta \langle v_{\text{eff}}^0 \rangle l, \quad (10)$$

in which the coefficient ζ does not depend on the external parameters and is equal to 0.3–0.4. Accordingly, for the streamer length as a function of the time we obtain from this

$$l(t) = r_0 \exp\{\zeta \langle v_{\text{eff}}^0 \rangle (t - t_0)\}. \quad (11)$$

The calculated time dependence of the streamer length is compared with the experiment of Ref. 9 (air at atmospheric pressure, $\lambda=10$ cm) in Fig. 4. We note that the field amplitude E_0 was not measured directly in Ref. 9, and therefore the value of E_0 for the calculation shown in the figure was chosen in such a way as to ensure the best agreement with the experiment. It can be seen that the exponential time dependence of the streamer length obtained in the calculations corresponds to the experiment. Proportionality of the

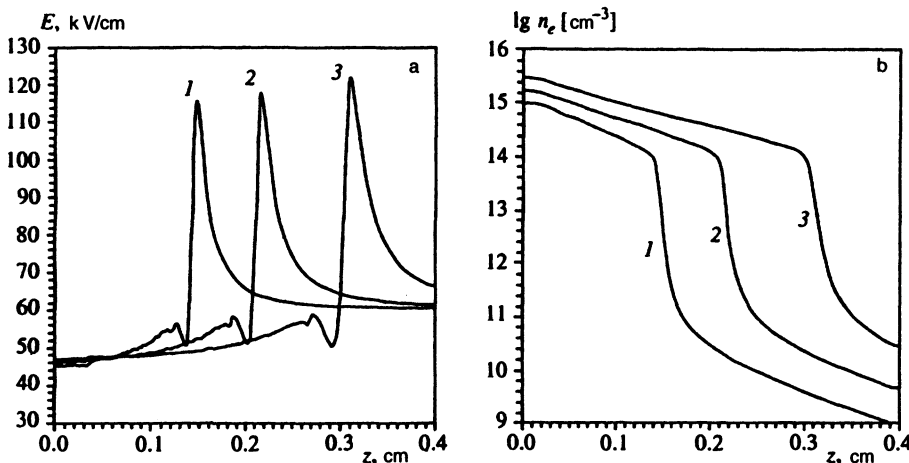


FIG. 2. Distributions of the amplitude of the electric field (a) and of the electron density (b) on the streamer axis under the conditions of Fig. 1 for $t=5.1$ (1), 5.7 (2), 6.3 ns (3).

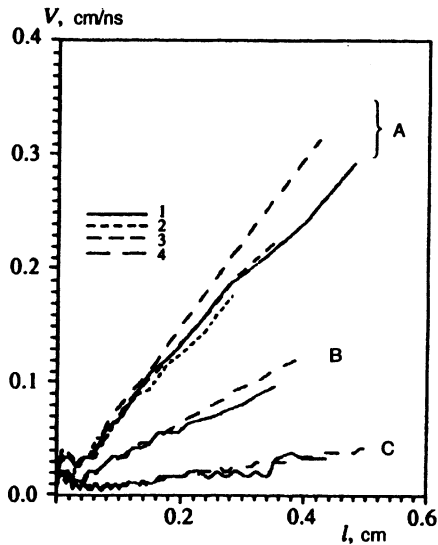


FIG. 3. Dependence of the streamer velocity on its length: $p_0=1$ atm; $E_0=60$ (A), 50 (B), 40 kV·cm (C). The curves 1, 2, and 3 correspond to the two-dimensional calculation for $r_0=0.02$ (1, 3) and 0.01 cm (2); $\lambda=9$ (1, 2) and 18 cm (3); curve 4 is the calculation in the 1D model.

streamer velocity to its length was also found in experimental¹⁰ and theoretical¹ investigations of streamer dynamics in homogeneous static fields.

We note that a calculation of streamer dynamics for the conditions of the experiment of Ref. 9 was made in Ref. 4 using the model proposed in Refs. 2 and 3, in which diffusion of charged particles was considered as the mechanism of discharge propagation. According to that calculation, photoionization plays the main role in the formation of the seeding electrons in front of the streamer head. Although diffusion is taken into account in the model, it plays a small role in the stage in which the field perturbation becomes appreciable. This conclusion also agrees with the results of

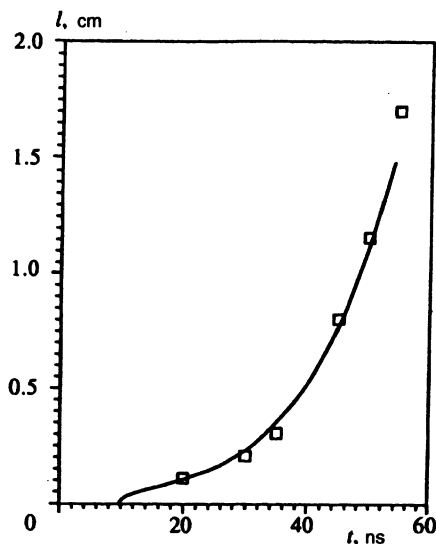


FIG. 4. Dependence of the streamer length on the time. The experimental points are taken from Ref. 9, and the curve is the calculation for $E_0=40$ kV/cm.

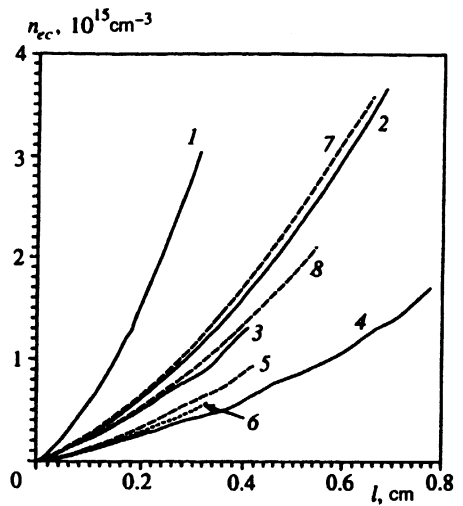


FIG. 5. Electron density at the center of the streamer: $p_0=1$ (1–5, 7, 8) and 0.5 atm (6); $\lambda=9$ (1–4, 6–8) and 18 cm (5); $E_0/p_0=60$ (1, 2, 4–7) and 50 kV·cm⁻¹·atm⁻¹ (3, 8); $r_0=0.01$ (1); 0.02 (2, 3, 5–8) and 0.04 cm (4). Curves 1–6 correspond to the two-dimensional calculation, and the curves 7 and 8 to the 1D calculation.

streamer calculations in homogeneous static fields (see Ref. 1).

Figure 5 shows the electron densities n_{ec} at the center of the streamer (at $z=r=0$). It can be seen that this variable can also be well described in the framework of the 1D model. The dependence of n_{ec} on the external parameters can be represented in the form

$$n_{ec} = n_{ei}(l/r_0)^\kappa, \quad (12)$$

where $n_{ei} = m\nu_m\omega/4\pi e^2$ is the value of the electron density at which the perturbation of the field becomes appreciable (ν_m is the frequency of momentum exchange between the electrons and the molecules), while the exponent κ in (12) increases from 1.0 to 1.3 as E_0/p_0 increases from 35 to 60 kV·cm⁻¹·atm⁻¹. For fixed streamer length, we find, in agreement with the results of the calculations $n_{ec} \sim p_0$, $n_{ec} \sim \omega \sim \lambda^{-1}$, $n_{ec} \sim r_0^{-\kappa}$.

Under the specified conditions, the main role in the kinetics of the electrons in the streamer channel is played by direct ionization. In the initial stage of the streamer development, recombination does not have a significant effect on the growth of n_{ec} . Estimates show that the role of step-by-step ionization is also small. Assuming that the growth of n_{ec} is described by the equation

$$\frac{dn_{ec}}{dt} = \langle \nu_{eff}^c \rangle n_{ec}, \quad (13)$$

where $\langle \nu_{eff}^c \rangle$ is the effective ionization frequency at the center of the streamer, we find from the relations (11)–(13) the connection between the frequencies of ionization in the applied field and in the field at the center of the streamer:

$$\langle \nu_{eff}^c \rangle / \langle \nu_{eff}^0 \rangle = \zeta \kappa = 0.3 - 0.5. \quad (14)$$

As can be seen from Fig. 1, in the region of the head of the streamer its transverse dimension (radius) increases with the length. The values of the streamer radius R_{str} , defined as

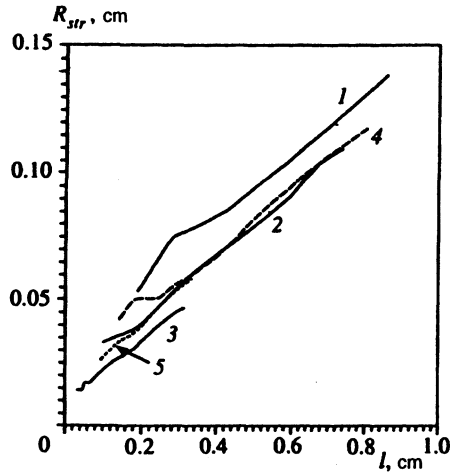


FIG. 6. Dependence of the streamer radius on its length: $\lambda=9$ cm; $p_0=1$ (1-4) and 0.5 atm (5); $E_0/p_0=60$ (1-3, 5) and 50 kV·cm $^{-1}$ ·atm $^{-1}$ (4); $r_0=0.04$ (1, 4), 0.02 (2, 5) and 0.01 cm (3).

the distance along r from the z axis to the position of the maximum of the radial component of the electric field in the widest part of the streamer (at $z \approx 0.8l$), are shown in Fig. 6. It can be seen that the streamer radius increases linearly with the length and that the slope of this dependence in all the forms of calculation has a constant value

$$\frac{dR_{\text{str}}}{dl} \approx 0.1. \quad (15)$$

In the theory of streamers, there is a well-known expression relating the streamer velocity to the ionization frequency $\langle \nu_{\text{eff}}^h \rangle$ in the head of the streamer and the radius of the head of the streamer:¹¹

$$V = \theta \langle \nu_{\text{eff}}^h \rangle R_{\text{str}}, \quad (16)$$

in which the coefficient θ is determined by the ratio of the electron densities ahead of and behind the head of the streamer. Figure 7 gives the values of $\langle \nu_{\text{eff}}^h \rangle R_{\text{str}}$ as functions of the streamer length. The nature of the dependence of this quantity on both the length and the external parameters is the same as for the streamer velocity, i.e., the relation (16) holds with coefficient $\theta=0.06-0.08$. For sufficiently long streamers, the growth of $\langle \nu_{\text{eff}}^h \rangle R_{\text{str}}$ with the length is due to the growth of the radius R_{str} , while the value of the field in the head and, therefore, the ionization frequency $\langle \nu_{\text{eff}}^h \rangle$ tend to saturation. It is interesting that linear growth of $\langle \nu_{\text{eff}}^h \rangle R_{\text{str}}$ with the streamer length also holds in the 1D model. However, in contrast to the two-dimensional case, in this model the streamer radius is constant, while the field in the head of the streamer increases with its length.

The relations (10) and (16) lead to an expression relating the values of the ionization frequency in the applied field and in the field in the head of the streamer:

$$\frac{\langle \nu_{\text{eff}}^h \rangle}{\langle \nu_{\text{eff}}^0 \rangle} = \frac{\xi l}{\theta R_{\text{str}}}. \quad (17)$$

In accordance with (15), for long streamers we have $l/R_{\text{str}} \sim 10$, and therefore the field saturation in the head of the

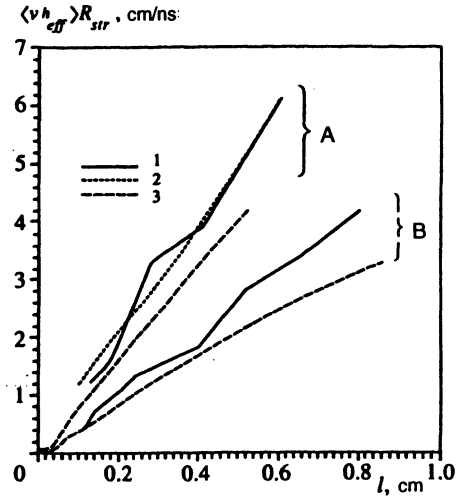


FIG. 7. Dependence of the product of the ionization frequency in the head of the streamer and its radius on the length of the streamer: $p_0=1$ atm; $\lambda=9$ cm; $E_0=60$ (A); 50 kV·cm (B); curves 1 and 2 give the two-dimensional calculation for $r_0=0.04$ (1) and 0.02 cm (2); curve 3 gives the result of the 1D calculation.

streamer occurs at a level corresponding to a ratio $\langle \nu_{\text{eff}}^h \rangle / \langle \nu_{\text{eff}}^0 \rangle \sim 40-60$ of the ionization frequencies. In reality, however, saturation can occur at streamer lengths comparable with the wavelength of the radiation, when the present approach becomes invalid.

The above relations, obtained on the basis of results of numerical calculations, make it possible to relate all the main characteristics of rf streamers in air (velocity, length, streamer radius, electron density, field strengths in the channel and in the streamer head) to the external parameters (strength and frequency of the applied field, pressure, initial size of the plasma region).

This work was done with the support of the International Science Foundation (Grant MHD000).

- ¹ P. A. Vitello, B. M. Penetrante, and J. N. Bardsley, *Phys. Rev. E* **49**, 5574 (1994).
- ² V. B. Gil'denburg, I. S. Gushchin, S. A. Dvinin, and A. V. Kim, *Zh. Éksp. Teor. Fiz.* **97**, 1151 (1990) [*Sov. Phys. JETP* **70**, 645 (1990)].
- ³ P. V. Vedenin and N. E. Rozanov, *Zh. Éksp. Teor. Fiz.* **105**, 868 (1994) [*JETP* **78**, 465 (1994)].
- ⁴ P. V. Vedenin and N. A. Popov, *Pis'ma Zh. Tekh. Fiz.* **20**, No. 13, 85 (1994) [*Tech. Phys. Lett.* **20**, 558 (1994)].
- ⁵ E. E. Kunhardt and C. Wu, *J. Comput. Phys.* **68**, 127 (1987).
- ⁶ J. W. Gallagher, E. C. Beaty, J. Dutton, and L. C. Pitchford, *J. Phys. Chem. Ref. Data* **12**, 109 (1983).
- ⁷ A. Kh. Mnatsakanyan and G. V. Naïdis, in *Plasma Chemistry*, No. 14 [in Russian, Énergoatomizdat, Moscow (1987)].
- ⁸ M. B. Zhelezniak, A. Kh. Mnatsakanyan, and S. V. Sisykh, *Teplofiz. Vys. Temp.* **20**, 423 (1982).
- ⁹ L. P. Grachev, I. I. Esakov, G. I. Mishin, and K. V. Khodataev, Preprint No. 1577 [in Russian] A. F. Ioffe Physicotechnical Institute (1992).
- ¹⁰ N. S. Rudenko and V. I. Smetanin, *Zh. Éksp. Teor. Fiz.* **61**, 146 (1971) [*Sov. Phys. JETP* **34**, 76 (1972)].
- ¹¹ M. I. D'yakonov and V. Yu. Kachorovskii, *Zh. Éksp. Teor. Fiz.* **94**, 321 (1988) [*Sov. Phys. JETP* **67**, 1049 (1988)]; **95**, 1850 (1989) [**68**, 1070 (1989)]; **98**, 895 (1990) [**71**, 498 (1990)].

Translated by Julian B. Barbour